NASA

Technical Memorandum 79627

Determining Crustal Strain Rates with a Spaceborne Geodynamics Ranging System

2. Station Coordinate Analysis

Steven C. Cohen and Glenn R. Cook

August 1978

National Aeronautics and
Space Administration

Goddard Space Flight Center
Greenbelt, Maryland 20771

TM 79627

DETERMINING CRUSTAL STRAIN RATES WITH A SPACEBORNE GEODYNAMICS RANGING SYSTEM, 2. STATION COORDINATE ANALYSIS

Steven C. Cohen
Glenn R. Cook
Geodynamics Branch
Goddard Space Flight Center
Greenbelt, Maryland 20771

August 1978

GODDARD SPACE FLIGHT CENTER
Greenbelt, Maryland

DETERMINING CRUSTAL STRAIN RATES WITH A SPACEBORNE GEODYNAMICS RANGING SYSTEM

2. STATION COORDINATE ANALYSIS

Steven C. Cohen
Glenn R. Cook
Geodynamics Branch
Goddard Space Flight Center

ABSTRACT

This paper is the second part of an analysis of the use of a Spaceborne Geodynamics Ranging System for determining crustal strain rates. The present analysis focuses on the use of site coordinates rather than intersite baseline distances for the strain rate determinations. After discussing the analytical techniques which are to be employed, numerical results are presented which suggest that the use of site coordinates would result in a 20-70% improvement in the precision of the deduced values of straining. Precisions of a few parts in 10^9 would be achievable with simple geometries and a decade or two of measurements; precisions of a few parts in 10^8 would be achievable in a few years. A consideration of possible correlations among the derived target site coordinates leads to the conclusion that, with the proper choice of coordinate systems, the correlations can be made small and non-detrimental to the strain rate determinations.

DETERMINING CRUSTAL STRAIN RATES WITH A SPACEBORNE GEODYNAMICS RANGING SYSTEM, 2. STATION COORDINATE ANALYSIS

1. INTRODUCTION

This paper continues an analysis of the use of the proposed Spaceborne Geodynamics Ranging System (SGRS) for determining crustal strain rates. This analysis was begun in an earlier paper (Cohen and Cook, 1978) herein referred to as Part 1. In Part 1 we outlined the basic measurement technique which would be employed by SGRS. The essense of that technique is a very precise determination of the locations of a number of targets situated on the ground. The survey is conducted by sequentially illuminating the reflective targets with a laser pulse from a device located onboard a spacecraft and measuring the times of flight for the laser pulses. These time of flights can be converted to ranges and with suitable knowledge of the spacecraft orbit, the earth's gravity field, and a number of other factors, the targets locations on the earth can be deduced. When the grid is resurveyed at a later date, changes in the target locations are interpreted in terms of crustal strain accumulation.

In Part 1 we analyzed the precision with which strain rates would be deduced from a consideration of changes in the baseline distances measured between the target sites. In the present paper we consider an alter-

native method of analysis based on the measurement of the changes in location of the sites themselves. This method more fully utilizes the information which could be extracted from a SGRS maasurement. As a consequence the deduced formal precisions are somewhat better and additional results, in the form of the target grid rotation rates, become available. Conversely, this method puts more stringent demands on the accuracy of the SGRS data since it depends on the vector resolution of relative intersite locations rather than the single parameter, intersite distance.

II. ANALYTIC CONSIDERATIONS

Strain is essentially a geometric concept. It is most easily visualized as a distortion of a line between nearby points. This distortion may be in the form of a change in the line length or a bending or both. Consider a continuous set of points described by the pairs of coordinates $(x, y,)$ in a two dimensional plane. Suppose that we start from an unstrained state and find that at some later time a point (x,y) has been displaced to a new location $(x+u, y+v)$. In general the displacements u and v are functions of the coordinates x and y. We can define certain components of an infinitesmal strain tensor by

$$\epsilon_{11} = \frac{\partial u}{\partial x} \qquad (1a)$$

$$\epsilon_{12} = \frac{\partial v}{\partial x} \qquad (1b)$$

$$\epsilon_{21} = \frac{\partial u}{\partial y} \qquad (1c)$$

$$\epsilon_{22} = \frac{\partial v}{\partial y} \qquad (1d)$$

(In Part 1 we used the symbols ϵ_x, ϵ_y, ϵ_{xy} for ϵ_{11}, ϵ_{12}, $\frac{1}{2}(\epsilon_{12}+\epsilon_{21})$).

It was shown in Part 1 that these components of the strain tensor can be re-

lated to a change in the distance between nearby points by

$$\epsilon \equiv \frac{r - r_o}{r_o} = \epsilon_{11} \cos^2 \theta + \dot{\epsilon}_{22} \sin^2 \theta + \tfrac{1}{2}(\epsilon_{12} + \epsilon_{21}) \cos \theta \sin \theta \qquad (2)$$

where r is the distance between the points in the strained state, r_o, is the unstrained distance, and θ is the angle the interlocation line makes with the positive x axis.

In general the unstrained state of the surveyed region is not known; rather the region is surveyed at different times to determine the rates of strain accumulation. Differentiating equation 2 we find

$$\dot{r} = r_o \left\{ \dot{\epsilon}_{11} \cos^2 \theta + \dot{\epsilon}_{22} \sin^2 \theta + \tfrac{1}{2}(\dot{\epsilon}_{12} + \dot{\epsilon}_{21}) \sin \theta \cos \theta \right\} \qquad (3)$$

Equation 3 suggests one method for determining strain rates. By determining changes in the lengths of three or more appropriately chosen lines in a region of homogeneous straining, the components of the two dimensional strain rate tensor can be deduced. We showed in Part 1 that with relatively simple site configurations, modest baselines of 25-70 km., and typical baseline precisions of a few centimeters, the strain rates could be determined to a precision of several parts in 10^9 in a measurement program lasting several years.

There are alternative procedures for deriving strain rates depending on the survey data available. In the present analysis we will assume that each of the target locations are known from the survey data in some conven-

ient reference frame; some discussion of the selection of the reference frame is presented later in this paper. Consider the x coordinate of two points (x_1, y_1) and $x_2, y_2)$. Assuming that the coordinate change linearly with time

$$x_1(t + \Delta t) - x_1(t) = \dot{u}(x_1, y_1)\,\Delta t \tag{4}$$

Furthermore to lowest order

$$\Delta\dot{u} = \dot{u}(x_2, y_2) - \dot{u}(x_1, y_1) = \frac{\partial \dot{u}}{\partial x}(x_2 - x_1) + \frac{\partial \dot{u}}{\partial y}(y_2 - y_1) \tag{5}$$

i. e. ,

$$\Delta\dot{u} = \dot{\epsilon}_{11}\,\Delta x + \dot{\epsilon}_{21}\,\Delta y \tag{6}$$

Similarly

$$\Delta\dot{v} = \dot{\epsilon}_{12}\Delta x + \dot{\epsilon}_{22}\Delta y \tag{7}$$

The preceding equations form the basis for the strain-rate analysis using station coordinates. Suppose as a result of several resurveys one has a collection of coordinates $(x_i(t_j), y_i(t_j))$ for several target locations at several times t_j then it is a straight forward matter to calculate $\dot{u}$ and $\dot{v}$. For example, using least square techniques if

$$x(t_j) = a + \dot{u}t_j \tag{8}$$

then for n measurements

$$\begin{bmatrix} a \\ \dot{u} \end{bmatrix} = \begin{bmatrix} n & \sum_1^n t_j \\ \sum t_j & \sum_1^n t_j^2 \end{bmatrix}^{-1} \begin{bmatrix} \sum_1^n x_i(t_j) \\ \sum_1^n x_i(t_j) t_j \end{bmatrix} \tag{9}$$

Given the rates $\dot{u}$ and $\dot{v}$ we can form differences $\Delta\dot{u}_i$, $\Delta\dot{v}_i$ for the rates between pairs of sites. Then if there are p pairs of target sites

$$\begin{bmatrix} \dot{\epsilon}_{11} & \dot{\epsilon}_{12} \\ \dot{\epsilon}_{21} & \dot{\epsilon}_{22} \end{bmatrix} = \begin{bmatrix} \sum_1^p \Delta x_i^2 & \sum_1^p \Delta x_i\, \Delta y_i \\ \sum_1^p \Delta x_i\, \Delta y_i & \sum_1^p \Delta y_i^2 \end{bmatrix}^{-1} \begin{bmatrix} \sum_1^p \Delta\dot{u}_i\, \Delta x_i & \sum_1^p \Delta\dot{v}_i\, \Delta x_i \\ \sum_1^p \Delta\dot{u}_i\, \Delta y_i & \sum_1^p \Delta\dot{v}_i\, \Delta y_i \end{bmatrix} \tag{10}$$

This equation should be discussed in some detail. The left hand side contains four components of a generalized strain rate tensor. We can write this tensor as a sum of a symmetric and antisymmetric tensor.

$$\begin{bmatrix} \dot{\epsilon}_{11} & \dot{\epsilon}_{12} \\ \dot{\epsilon}_{21} & \dot{\epsilon}_{22} \end{bmatrix} = \begin{bmatrix} \dot{\epsilon}_{11} & \tfrac{1}{2}(\dot{\epsilon}_{12} + \dot{\epsilon}_{21}) \\ \tfrac{1}{2}(\dot{\epsilon}_{12} + \dot{\epsilon}_{21}) & \dot{\epsilon}_{22} \end{bmatrix} + \begin{bmatrix} 0 & \tfrac{1}{2}(\dot{\epsilon}_{12} - \dot{\epsilon}_{21}) \\ -\tfrac{1}{2}(\dot{\epsilon}_{12} - \dot{\epsilon}_{21}) & 0 \end{bmatrix} \tag{11}$$

The symmetric tensor is the pure strain rate tensor discussed in Part 1, while the antisymmetric tensor represents a rotation rate.

Next we note that the inverse matrix on the left side of equation 10 gives the geometric contribution to the variance-covariance matrix for the strain rate determination. When multiplied by the variance in the coordinate rate differences, the diagonal terms give the variances in the strain rates and the off-diagonal terms give the covariances between terms. Let

$$A = \begin{bmatrix} \Delta x_1 & \Delta y_1 \\ \Delta x_2 & \Delta y_2 \\ \vdots & \vdots \\ \Delta x_p & \Delta y_p \end{bmatrix} \tag{12}$$

then the inverse matrix is $(A^T A)^{-1}$ and

$$(A^T A)^{-1} = \frac{1}{\left\{\sum_1^p \Delta x_i^2 \sum_1^p \Delta y_i^2 - (\sum_1^p \Delta x_i \Delta y_i)^2\right\}} \begin{bmatrix} \sum_1^p \Delta y_i^2 & -\sum_1^p \Delta x_i \Delta y_i \\ -\sum_1^p \Delta x_i \Delta y_i & \sum_1^p \Delta x_i^2 \end{bmatrix} \tag{13}$$

$$= \frac{1}{\left\{\sum_1^p (r_{o_i} \ell_i)^2 \sum_1^p (r_{o_i} m_i)^2 - \sum_1^p (r_{o_i}^2 \ell_i m_i)^2\right\}} \begin{bmatrix} \sum_1^p (r_{o_i} m_i)^2 & -\sum_1^p (r_{o_i}^2 \ell_i m_i) \\ -\sum_1^p (r_{o_i}^2 \ell_i m_i) & \sum_1^p (r_{o_i} \ell_i)^2 \end{bmatrix}$$

where the r_{o_i} are intersite distances and the ℓ_i and m_i are direction cosines with respect to the x and y axes respectively. Let $\sigma^2_{\Delta \dot{u}}$ and $\sigma^2_{\Delta \dot{v}}$ be the variances in $\Delta \dot{u}$ and $\Delta \dot{v}$ and $\sigma^2_{\Delta x}$ and $\sigma^2_{\Delta y}$ be the corresponding variances in Δx and Δy. From equation 9

$$\sigma^2_{\Delta \dot{u}} = \frac{n}{n\sum_1^n t_j^2 - (\sum_1^n t_j)^2} \sigma^2_{\Delta x} \tag{14}$$

The variances in the strain rates can be calculated from equations 13 and 14,

$$\sigma^2_{\dot{\epsilon}_{11}} = (A^T A)^{-1}_{11} \sigma^2_{\Delta \dot{u}} \tag{15a}$$

$$\sigma^2_{\dot{\epsilon}_{12}} = (A^T A)^{-1}_{11} \sigma^2_{\Delta \dot{v}} \tag{15b}$$

$$\sigma^2_{\dot{\epsilon}_{21}} = (A^T A)^{-1}_{22} \sigma^2_{\Delta \dot{u}} \tag{15c}$$

$$\sigma^2_{\dot{\epsilon}_{22}} = (A^T A)^{-1}_{22} \sigma^2_{\Delta \dot{v}} \tag{15d}$$

Furthermore if we assume $\dot{\epsilon}_{12}$ and $\dot{\epsilon}_{21}$ are uncorrelated the variance in the shear strain is $\frac{1}{2}(\sigma^2_{\dot{\epsilon}_{12}} + \sigma^2_{\dot{\epsilon}_{21}})$ which is also the variance in the rotation rate.

In the next section we will present results showing the expected standard deviations in the strain rate determinations. These values are simply the square roots of the preceding variances.

III. RESULTS

The precision with which the strain rates can be deduced depends on the geometry of the target grid, the number of sites, the resurvey period, Δt, the period between the first and last measurements, T, and, of course, the precision in the deduced site locations. In Figure 1 we show five simple target grids for which we have calculated the expected precision using the present analysis and which we also used in Part 1 for that analysis. The results of our calculations are shown in Figures 2-6. These results have been normalized to a one centimeter standard deviation in the difference in site coordinates, a normalization consistent with the one centimeter standard deviation in baseline distances used in Part 1. (If we assume that all coordinates are determined to the same precision and are uncorrelated then, for example, $\sigma_{\Delta x} = \sigma_r = \sqrt{2}\,\sigma_x$.) For the simple triangle of Figure 1a the precision in the deduced strain rates improves from about 2 parts in 10^7 per year after two years to 1-3 parts in 10^8 per year after 15 years. These numbers should be compared to the typical rates of straining on, say, the San Andreas Fault of a few parts in 10^7 per year. Considerable improvements in the precision can be obtained

by going to grids involving more than three targets. For the 9 target grid of Figure 1e, the precision varies from about 4 parts in 10^8 per year after two years to 2-3 parts in 10^9 after fifteen years.

It is interesting to compare the results obtained here using site coordinates with those obtained from a baseline distance analysis. Such a comparision is shown in Table 1. The principal strain rates, $\dot{\epsilon}_{11}$ and $\dot{\epsilon}_{22}$, derived from the coordinates are typically 20 percent more precise than those obtained using baselines. The shear strain rate precisions improve by a factor 1.4-1.7 in going from the baseline to coordinate analysis. Furthermore the relative precision in the deduced values of the components of the strain rate tensor may vary with the method of analysis. For Figure 1d the precision in is twice that of $\dot{\epsilon}_{22}$ in the site coordinate analysis but $\sqrt{6}$ better in the baseline distance analysis.

We have assumed in the analysis presented here and in Part 1 that the correlations in the deduction of various components of several site locations are negligible. We should consider this point in a bit more detail. If positive correlations exist among common components, say the x component, of different station locations, then the measurement and analysis errors give rise to a common position bias which is largely removed when the differences between target locations are determined in either of the analysis methods we have considered. On the other hand if the correlations are large and negative, the precisions can be substantially degraded. We examine the question of

correlations by considering a variance-covariance matrix P for the site locations. Let

$$S = \begin{bmatrix} \delta x_1 \\ \delta y_1 \\ \delta x_2 \\ \delta y_2 \\ \vdots \\ \delta x_p \\ \delta y_p \end{bmatrix} \tag{16}$$

be the vector of uncertainties in the site locations. The matrix P is defined by

$$P = \langle SS^T \rangle \tag{17}$$

Associated with the variance-covariance matrix is a correlation matrix, with definition

$$\rho_{ij} = P_{ij}/(P_{ii}P_{jj})^{1/2} \tag{18}$$

The diagonal elements of the correlation matrix have a value of unity while the values of the off-diagonal terms vary from +1 (fully correlated) to -1 (fully correlated negatively) with the value 0 corresponding to no correlation. If the quantities α and β have a correlation $\rho_{\alpha\beta}$ then

$$\sigma^2_{\alpha\pm\beta} = \sigma^2_\alpha + \sigma^2_\beta \pm 2\rho\sigma_\alpha\sigma_\beta. \tag{19}$$

In order to develop a quantitative appreciation for the correlations we consider a network of nine stations which are part of a larger grid being

considered for part of California. The coordinates for the targets are shown in Table 2; the arrangement of sites is similar to that of Figure 1e although the sides of the grid are not along East-West and North-South lines. The expected precisions in site locations and the correlations among coordinates have been considered in two separate coordinate systems. The first system is an earth center fixed coordinate system (ECF) in which the z axis is aligned with the Earth's rotation axis, the x axis points toward the prime meridian through Greenwich and the y axis completes a right handed orthogonal system. The second system is a local tangent plane coordinate system (LTP) with one of the target sites held fixed at the origin. In this system the x axis points to the East and the y axis to the North. The z axis is vertical. The mean values of the correlations determined in each of these two systems are shown in Table 3. (Not shown are the r.m.s precisions in the position determinations which are typically 11 cm. for each component in the ECF system and about 2 cm. for each component in the LTF system.) On comparing these results we conclude that the bulk of the errors in the site locations in the ECF system are bias errors which are partially removed by transforming to the LTP system.

In the LTP system mean values of the correlations are less than 0.3 except in the vertical direction. It may be significant to note that the correlations among the x and y components have nearly zero means while the correlations between common components of different stations still have a positive mean. This suggest

the presence of a residual bias which might be removed by transforming to a new coordinate system with a resultant further improvement in the precision. For the purposes of this paper, however, the correlations are already sufficiently small to suggest that our deductions concerning strain rate precisions should be correct to with a factor of two or so.

IV CONCLUSIONS

We have considered the potential use of measurements made with a SGRS system for determining crustal strain rates. In Part 1 a method of analysis was outlined which focused on the use intersite distance measurements while in Part 2 the method relied on a decomposition of the intersite vector into relative coordinates. Numerical calculations using small target grids with 25–70 km site separations suggest that straining rates can be determined to a few parts in 10^8 per year, after several years. Precisions of several parts in 10^9 may be attainable with a decade or so of measurements. The use of station coordinates as opposed to baseline distances result in a modest improvement in the precision of the derived strain rates as well as permitting more detailed decomposition of the strain rate tensor.

ACKNOWLEDGMENTS

We wish to thank Werner Kahn for his many contributions to our understanding of the SGRS system and its potential capabilities. We also thank him and Tom Engler for providing us with the covariance matrix for site coordinates prior to its publication.

REFERENCES

Cohen, S. C., and G. R. Cook, "Determining Crustal Strain with a Spaceborne Geodynamics Ranging System 1, Baseline Analysis, NASA-Goddard Space Flight Center TM-79565, June 1978

TABLE 1

Relative Standard Deviations in Strain Rate Determinations Based on Relative Site Coordinates, σ_c, and Intersite Baseline Distances, σ_b.

	Component		
Figure no.	$\dot{\epsilon}_{11}$	$\dot{\epsilon}_{22}$	$\frac{1}{2}(\dot{\epsilon}_{12} + \dot{\epsilon}_{21})$
1a	$\sigma_b/\sigma_c = 1.2$	$\sigma_b/\sigma_c = 1.2$	$\sigma_b/\sigma_c = 1.7$
1b	1.2	1.2	1.7
1c	1.2	1.2	1.4
1d	1.1	1.3	1.4
1e	1.2	1.2	1.5

TABLE 2

Station number	Longitude	Latitude	Elevation (m)
151	119°57'	36°01'	61
152	119°46'	35°50'	304
153	119°36'	35°40'	910
161	120°10'	35°52'	305
162	119°59'	35°42'	215
163	119°48'	35°31'	152
171	120°23'	35°43'	457
172	120°11'	35°32'	609
173	120°00'	35°22'	610

TABLE 3

Correlation coefficients associated with off diagonal terms of coordinate covariance matrix calculated for a nine station subnetwork of proposed California grids. Station 162 is the fixed station for calculations in the LTP system.

		ECF Coordinate System		LTP Coordinate System	
Component		$\langle\rho\rangle$	$\langle(\rho-\langle\rho\rangle^2)\rangle^{1/2}$	$\langle\rho\rangle$	$\langle(\rho-\langle\rho\rangle)^2\rangle^{1/2}$
$x_i x_j$	$i \neq j$	.97	.02	.27	.37
$y_i y_j$		.98	.01	.29	.32
$z_i z_j$		.99	.01	.48	.01
$x_i y_j$		.06	.08	.02	.35
$x_i z_j$		.08	.09	.09	.02
$y_i z_j$		.36	.04	-.09	.02
$x_i y_i$		.06	.07	-.00	.24
$x_i z_i$		.09	.09	.19	.08
$y_i z_i$		.36	.06	-.17	.04

FIGURE CAPTIONS

Figure 1. Representative SGRS target site grids.

Figure 2. Calculated precision in the strain rates $\dot{\epsilon}_{11}$, $\dot{\epsilon}_{21}$, $\dot{\epsilon}_{12}$, $\dot{\epsilon}_{22}$ for the grid shown in Figure 1a.

Figure 3. Calculated precision in the strain rates $\dot{\epsilon}_{11}$, $\dot{\epsilon}_{21}$, $\dot{\epsilon}_{12}/2$, $\dot{\epsilon}_{22}/2$ for the grid shown in Figure 1b.

Figure 4. Calculated precision in the strain rates $\dot{\epsilon}_{11}$, $\dot{\epsilon}_{21}$, $\dot{\epsilon}_{12}$, $\dot{\epsilon}_{22}$ for the grid shown in Figure 1c.

Figure 5. Calculated precision in the strain rates $\dot{\epsilon}_{11}$, $\dot{\epsilon}_{21}$, $\dot{\epsilon}_{12}/2$, $\dot{\epsilon}_{12}/2$ for the grid shown in Figure 1d.

Figure 6. Calculated precision in the strain rates $\dot{\epsilon}_{11}$, $\dot{\epsilon}_{21}$, $\dot{\epsilon}_{12}$, $\dot{\epsilon}_{22}$ for the grid shown in Figure 1e.

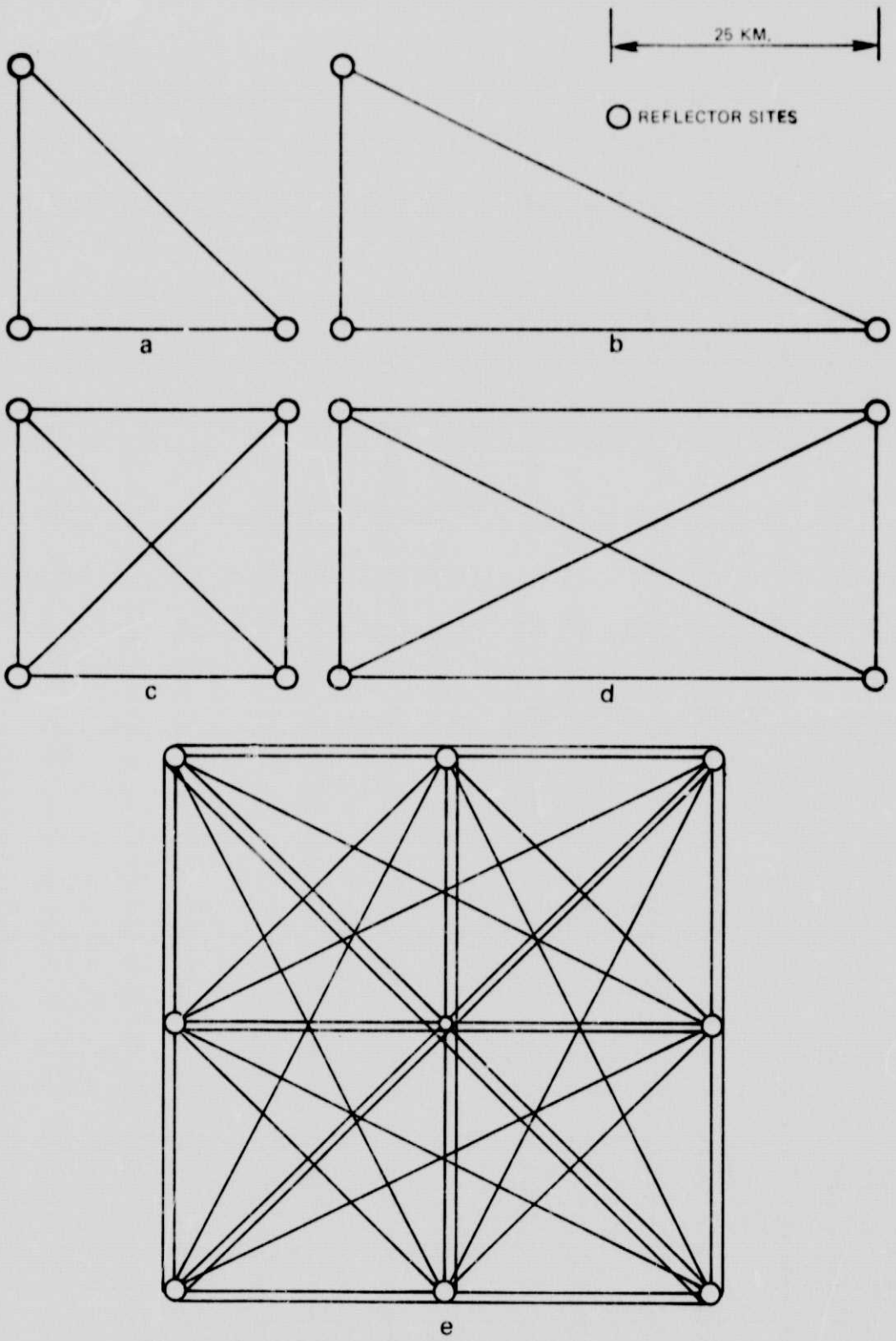

Figure 1. Representative SGRS target site grids

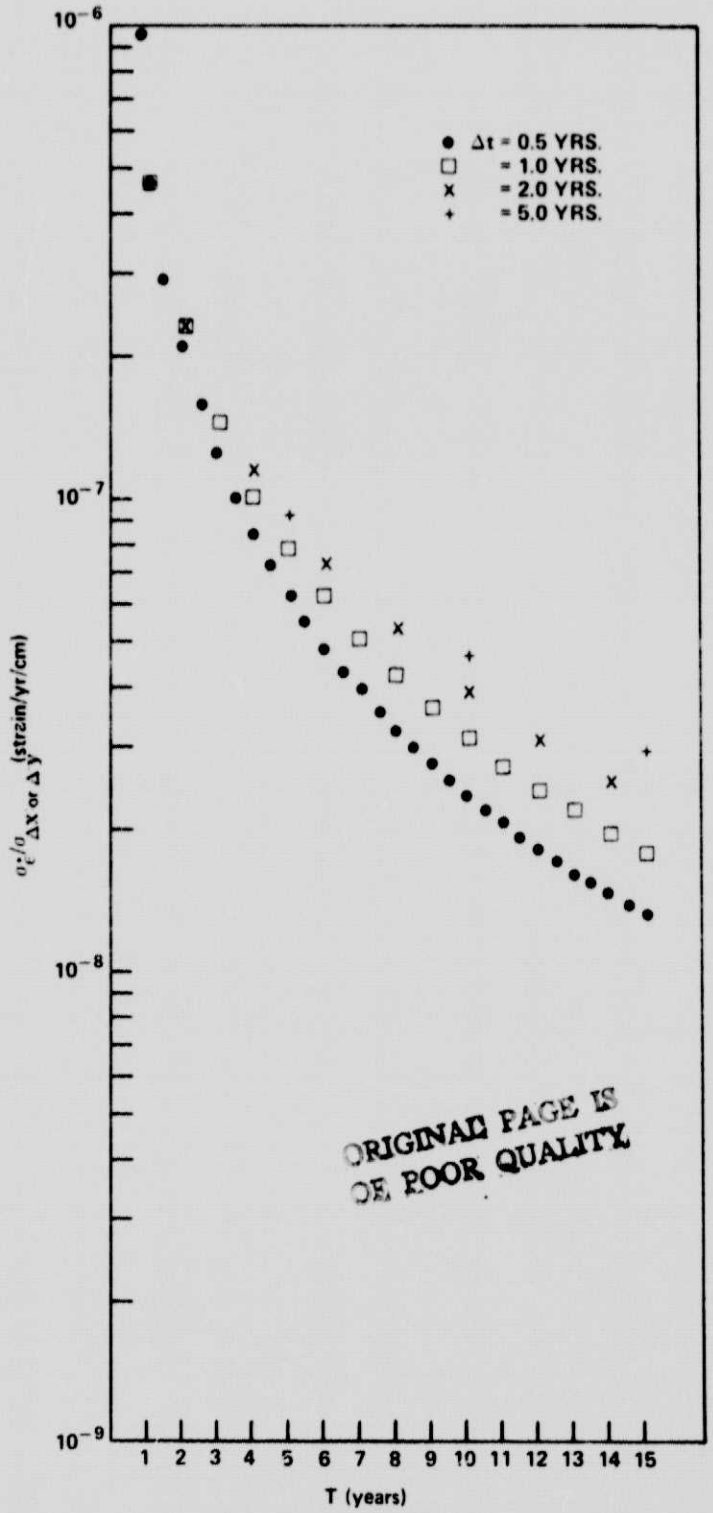

Figure 2. Calculated precision in the strain rates $\dot{\epsilon}_{11}$, $\dot{\epsilon}_{21}$, $\dot{\epsilon}_{12}$, $\dot{\epsilon}_{22}$ for the grid shown in Figure 1a

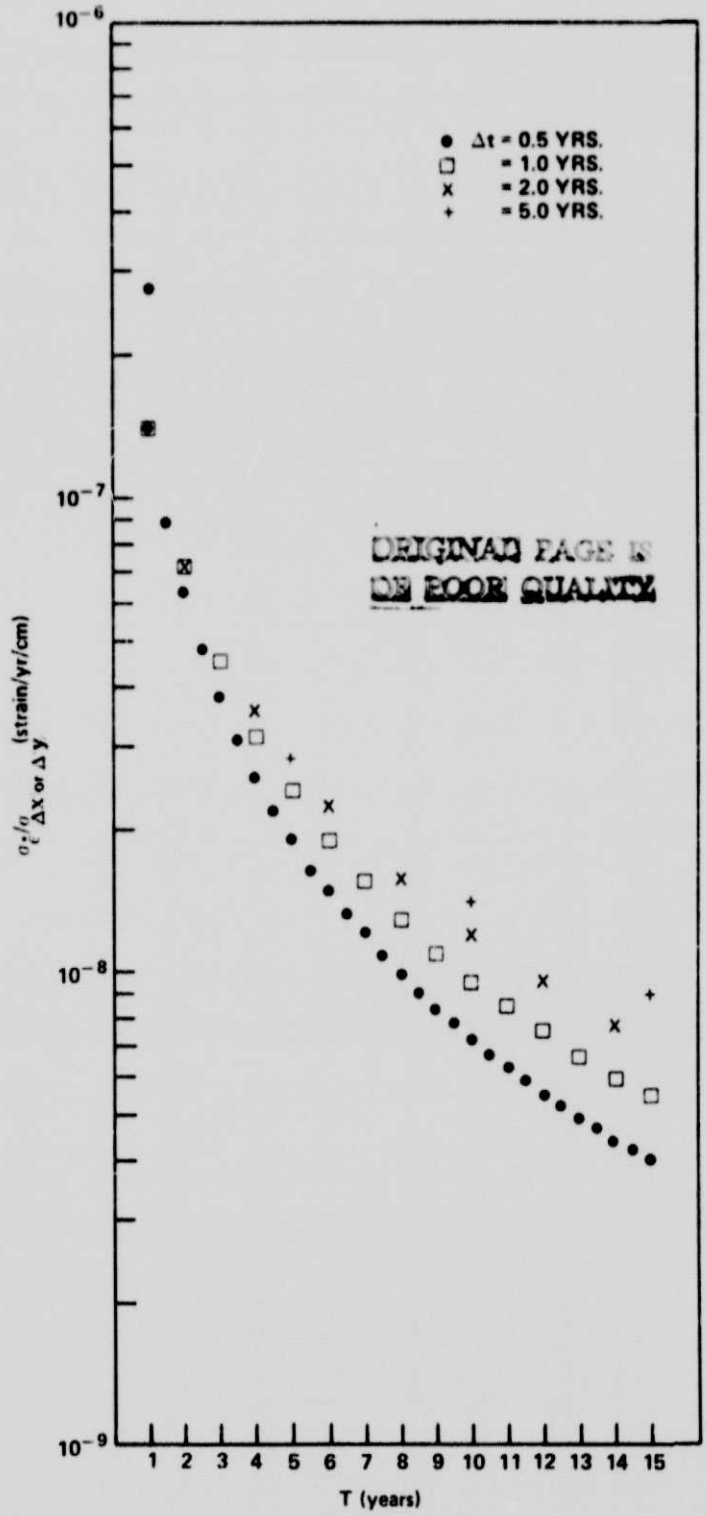

Figure 3. Calculated precision in the strain rates $\dot{\epsilon}_{11}$, $\dot{\epsilon}_{21}$, $\dot{\epsilon}_{12}/2$, $\dot{\epsilon}_{22}/2$ for the grid shown in Figure 1b

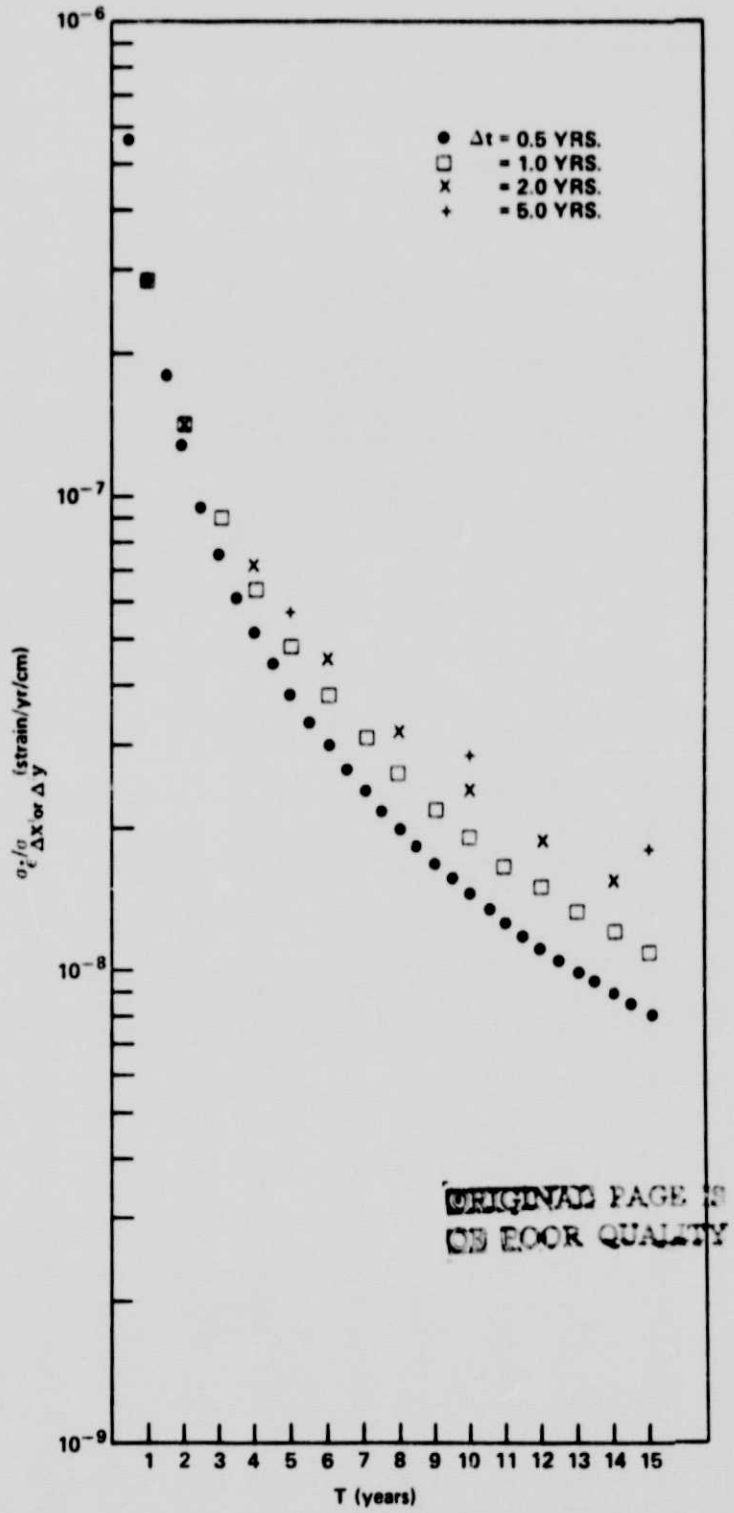

Figure 4. Calculated precision in the strain rates $\dot{\epsilon}_{11}$, $\dot{\epsilon}_{21}$, $\dot{\epsilon}_{12}$, $\dot{\epsilon}_{22}$ for the grid shown in Figure 1c

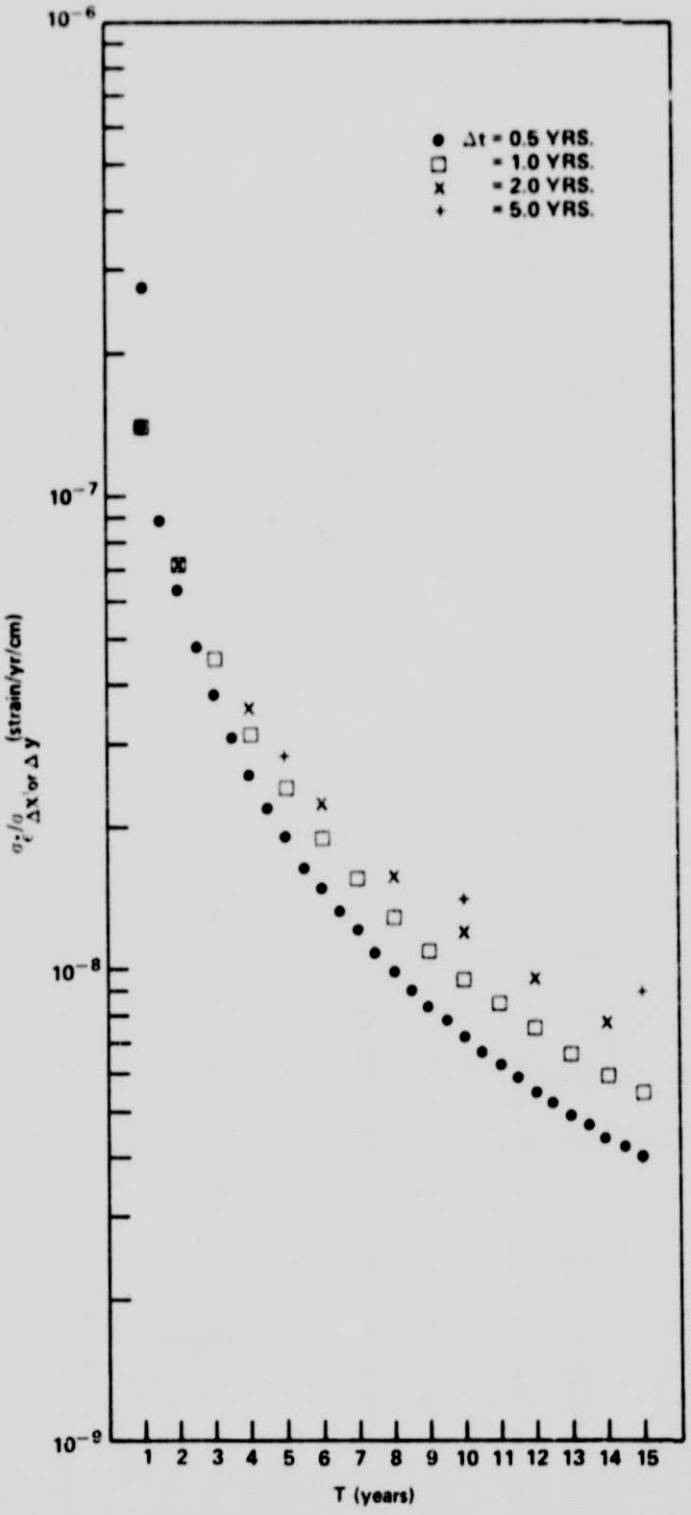

Figure 5. Calculated precision in the strain rates $\dot{\epsilon}_{11}$, $\dot{\epsilon}_{21}$, $\dot{\epsilon}_{12}/2$, $\dot{\epsilon}_{22}/2$ for the grid shown in Figure 1d

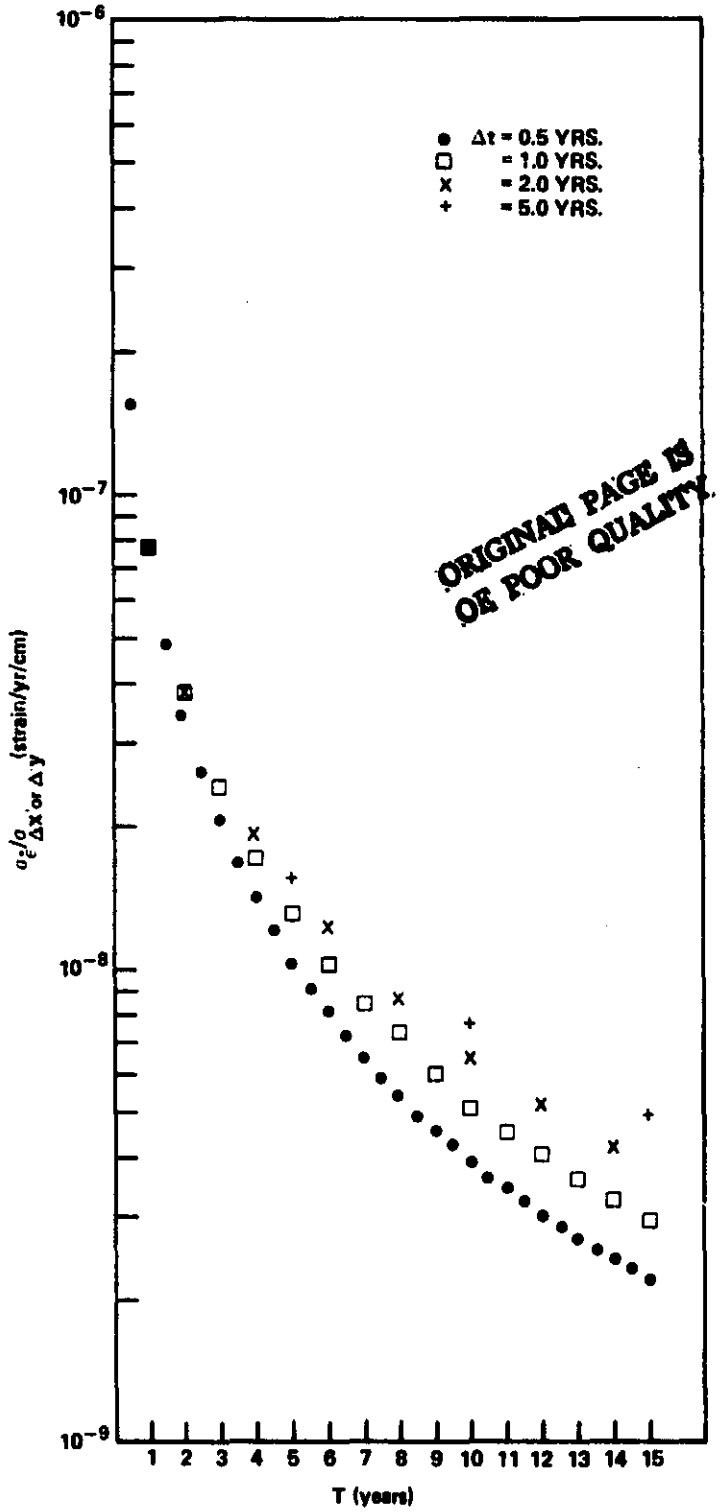

Figure 6. Calculated precision in the strain rates $\dot{\epsilon}_{11}$, $\dot{\epsilon}_{21}$, $\dot{\epsilon}_{12}$, $\dot{\epsilon}_{22}$ for the grid shown in Figure 1e